

**DESY 94-207**  
**MZ-TH/94-28**  
**TTP 94-20**  
**hep-ph/9411372**  
 November 1994

## INELASTIC $J/\psi$ PHOTOPRODUCTION \*

M. Krämer<sup>a†</sup>, J. Zunft<sup>b</sup>, J. Steegborn<sup>c</sup>, and P. M. Zerwas<sup>b</sup>

<sup>a</sup>Inst. Physik, Johannes Gutenberg-Universität, D-55099 Mainz FRG

<sup>b</sup>Deutsches Elektronen-Synchrotron DESY, D-22603 Hamburg FRG

<sup>c</sup>Inst. Theor. Teilchenphysik, Univ. Karlsruhe, D-76128 Karlsruhe FRG

### ABSTRACT

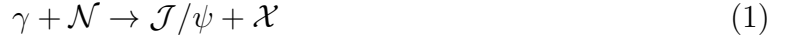
Inelastic photoproduction of  $J/\psi$  particles at high energies is one of the processes to determine the gluon distribution in the nucleon. We have calculated the QCD radiative corrections to the color-singlet model of this reaction. They are large at moderate photon energies, but decrease with increasing energies. The cross section and the  $J/\psi$  energy spectrum are compared with the available fixed-target photoproduction data and predictions are given for the HERA energy range.

\* Supported in part by Deutsche Forschungsgemeinschaft DFG

† Present address: Deutsches Elektronen-Synchrotron DESY, D-22603 Hamburg FRG;

E-mail: [mkraemer@vxdesy.desy.de](mailto:mkraemer@vxdesy.desy.de)

The measurement of the gluon distribution in the nucleon is one of the important goals of lepton-nucleon scattering experiments. The classical methods exploit the evolution of the nucleon structure functions with the momentum transfer, and the size of the longitudinal structure function. With rising energies, however, jet physics and the production of heavy quark states become important complementary tools. Besides open charm and bottom production, the formation of  $J/\psi$  bound states [1] in inelastic photoproduction experiments



provides an experimentally attractive method since  $J/\psi$  particles are easy to tag in the leptonic decay modes.

Many channels contribute to the generation of  $J/\psi$  particles in photoproduction experiments [2], similarly to hadroproduction experiments. However, no satisfactory quantitative picture has emerged yet and the production of a large surplus of  $\psi'$  particles in  $p\bar{p}$  collisions awaits the proper understanding. Theoretical interest so far has focussed on two mechanisms for  $J/\psi$  photo- and electroproduction, elastic/diffractive [3,4] and inelastic production through photon-gluon-fusion [1,2]. While by the first mechanism one expects to shed light on the physical nature of the pomeron, inelastic  $J/\psi$  production provides information on the distribution of gluons in the nucleon [5]. The two mechanisms can be separated by measuring the  $J/\psi$  energy spectrum, described by the scaling variable

$$z = \frac{p k_\psi}{p k_\gamma} \quad (2)$$

with  $p, k_{\psi, \gamma}$  being the momenta of the nucleon and  $J/\psi, \gamma$  particles, respectively. In the nucleon rest frame,  $z$  is the ratio of the  $J/\psi$  to the  $\gamma$  energy,  $z = E_\psi/E_\gamma$ . For elastic/diffractive events  $z$  is close to one; the inelastic events are experimentally restricted in general to the range  $z < 0.9$  [6]. The production of  $J/\psi$  particles at large transverse momenta is dominated by gluon fragmentation mechanisms [7].

Inelastic  $J/\psi$  photoproduction through photon-gluon fusion is described in the color-singlet model<sup>1</sup> through the subprocess



shown in Fig.1. Color conservation and the Landau-Yang theorem require the emission of a gluon in the final state. The cross section is generally calculated in the static approximation in which the motion of the charm quarks in the bound state is neglected. In this approximation the production amplitude factorizes into the short distance amplitude  $\gamma + g \rightarrow c\bar{c} + g$ , with  $c\bar{c}$  in the color-singlet state and zero relative velocity of the quarks, and the  $c\bar{c}$  wave function  $\varphi(0)$  of the  $J/\psi$  bound state at the origin which is related to the leptonic width. The cross section of the subprocess (3) may be written as

$$\frac{d\sigma^{(0)}}{dt_1} = \frac{128\pi^2}{3} \frac{\alpha\alpha_s^2 e_c^2}{s^2} M_{J/\psi}^2 \frac{|\varphi(0)|^2}{M_{J/\psi}} \frac{s^2 s_1^2 + t^2 t_1^2 + u^2 u_1^2}{s_1^2 t_1^2 u_1^2} \quad (4)$$

---

<sup>1</sup>Dual approaches to  $J/\psi$  photoproduction based on the subprocess  $\gamma + g \rightarrow c + \bar{c}$  are, in contrast to their  $e^+e^-$  analogon, not sharply defined and they will therefore not be discussed in the present context.

where  $t$  denotes the momentum transfer squared from the photon to the  $J/\psi$  particle, and  $s, u$  are the total energy and the momentum transfer from the photon to the gluon [ $t_1 = t - M_{J/\psi}^2$  etc.]. The cross section (4) is infrared finite. The photoproduction cross section on the nucleon is obtained by integrating the subprocess over the gluon flux,

$$\sigma = \int d\xi g(\xi) \hat{\sigma} \quad (5)$$

When confronted with photoproduction data of fixed-target experiments [8,9], the theoretical predictions underestimate the measured cross section in general by more than a factor two, depending in detail on the  $J/\psi$  energy and the choice of the parameters [for a recent review see Ref. [2]]. The discrepancy with cross sections extrapolated from electroproduction data [10,11] is even larger.

The lowest-order approach to the color-singlet model demands several theoretical refinements: (i) Higher-order perturbative QCD corrections; (ii) Relativistic corrections due to the motion of the charm quarks in the  $J/\psi$  bound state; and last but not least, (iii) Higher-twist effects which are not strongly suppressed due to the fairly low charm-quark mass. While the relativistic corrections have recently been demonstrated to be under control in the inelastic region [12], the problem of higher-twist contributions has not been approached so far. The analysis of the higher-order perturbative QCD corrections will be presented in this note. Expected *a priori* and verified subsequently, these corrections by far dominate the relativistic corrections in the inelastic region, being of the order of several  $\alpha_s(M_{J/\psi}^2) \sim 0.3$ . In the first step of a systematic expansion, they can therefore be determined in the static approach [13].

Generic diagrams which build up the cross section in next-to-leading order are depicted in Fig.1. Besides the usual self-energy diagrams and vertex corrections for photon and gluons (b), we encounter box diagrams (c), the splitting of the final-state gluon into gluon and light quark-antiquark pairs, as well as diagrams renormalizing the initial-state parton densities (e). The evaluation of these amplitudes has been performed in the Feynman gauge. We have adopted the dimensional regularization scheme to calculate the singular parts of the amplitudes. [We have refrained from using the seemingly simpler scheme of dimensional reduction which however gives rise to complications in the massive quark case as pointed out in Ref. [14].] The masses of light quarks in Fig.1(d,e<sub>1</sub>) have been neglected while the mass parameter of the charm quark has been defined on-shell, with  $m_c = \frac{1}{2}M_{J/\psi}$  for consistency. Since the proper renormalization scale  $\mu_R$  is expected in the range of about  $m_c$  to  $M_{J/\psi} = 2m_c$ , we have used the  $\overline{MS}$  scheme [15] with four active flavors for the renormalization of the QCD coupling  $\alpha_s^{(n_f)}(\mu_R^2)$ . We have carried out the renormalization program also in the *extended*  $\overline{MS}$  scheme [16] in which the massive particles are decoupled smoothly for momenta smaller than the quark mass. The results in the two schemes differ marginally, by typically less than 6 %. The exchange of Coulombic gluon quanta in the diagram (1c) leads to a Coulomb singularity  $\sim \pi^2/2\beta_R$  which can be isolated by introducing a small relative quark velocity  $\beta_R$ . Following the standard path [17], we interpret this effect as Sommerfeld rescattering correction which can effectively be mapped into the  $c\bar{c}$  wave function. As expected, the infrared singularities cancel when the emission of soft and collinear final-state gluons and light quarks, characterized by a cut-off  $\Delta$  [14,18], is added to the virtual corrections. The collinear initial-state singularities can be absorbed, as usual, into the renormalization of the parton densities [19] defined in the  $\overline{MS}$  factorization scheme.

After carrying out this straightforward but tedious program, the results for the cross sections of the subprocesses can be presented in the form of scaling functions,

$$\hat{\sigma}_{i\gamma}(s, m_c^2) = \frac{\alpha \alpha_s^2 e_c^2}{m_c^2} \frac{|\varphi(0)|^2}{m_c^3} \left[ c_{i\gamma}^{(0)}(\eta) + 4\pi \alpha_s \left\{ c_{i\gamma}^{(1)}(\eta) + \bar{c}_{i\gamma}^{(1)}(\eta) \ln \frac{Q^2}{m_c^2} \right\} \right] \quad (6)$$

$i = g, q, \bar{q}$  denoting the parton targets. For the sake of simplicity, we have identified the renormalization scale with the factorization scale  $\mu_R^2 = \mu_F^2 = Q^2$ . The scaling functions depend on the energy variable  $\eta = s/4m_c^2 - 1$ .  $c_{\gamma g}^{(0)}$  is the lowest-order contribution which scales  $\sim \eta^{-1} \sim 4m_c^2/s$  asymptotically.  $c_{\gamma g}^{(1)}$  can be decomposed into a "virtual + soft" (V+S) piece, and a "hard" (H) gluon-radiation piece; the  $\ln^j \Delta$  singularities of the (V+S) cross section are mapped into (H), cancelling the equivalent logarithms in this contribution so that the limit  $\Delta \rightarrow 0$  can safely be carried out [18]. The *nomenclatura* "hard" and "virtual + soft" is therefore a matter of definition, and negative values of  $c^{(H)}$  may occur in some regions of the parameter space. Up to this order, the wave-function at the origin is related to the leptonic  $J/\psi$  width by

$$\Gamma_{ee} = \left(1 - \frac{16}{3} \frac{\alpha_s}{\pi}\right) \frac{16\pi\alpha^2 e_c^2}{M_{J/\psi}^2} |\varphi(0)|^2 \quad (7)$$

with only transverse gluon corrections taken into account explicitly [20].

The scaling functions  $c_{\gamma i}(\eta)$  are shown in Figs.2a/b for the parton cross sections integrated over  $z \leq z_1$  where we have chosen  $z_1 = 0.9$  as discussed before. [Note that the definition of  $z$  is the same at the nucleon and parton level since the momentum fraction  $\xi$  of the partons cancels in the ratio (2).] The following comments can be inferred from the figures. (i) The form of the scaling functions resembles the scaling functions in open-charm photoproduction [18]. However, there is an important difference. The "virtual + soft" contribution for  $J/\psi$  production is significantly more negative than for open-charm production. The destructive interference with the lowest-order amplitude is not unphysical though, as the momentum transfer of virtual gluons has a larger chance [in a quasi-classical approach] to scatter quarks out of the small phase-space element centered at  $p_c + p_{\bar{c}} = p_{J/\psi}$  than to scatter them from outside into this small element. (ii) While  $c_{\gamma g}^{(0)}$  and  $c_{\gamma g}^{(1,V+S)}$  scale asymptotically  $\sim 1/s$ , the hard coefficients  $c_{\gamma g}^{(1,H)}$  and  $c_{\gamma q}^{(1)}$  [as well as  $\bar{c}_{\gamma g}^{(1)}$ ] approach plateaus for high energies, built-up by the flavor excitation mechanism. (iii) The cross sections on the quark targets are more than one order of magnitude smaller than those on the gluon target. (iv) A more detailed presentation of the spectra would reveal that the perturbative analysis is not under proper control in the limit  $z \rightarrow 1$ , as anticipated for this singular boundary region [21]. Outside the diffractive region, i.e. in the truly inelastic domain, the perturbation theory is well-behaved however.

The cross sections for  $J/\psi$  photoproduction on nucleons are presented in Figs.3a and 3b. In the first of the two figures we compare the leading-order and next-to-leading order calculations with the  $J/\psi$  energy spectra of the two fixed-target photoproduction experiments at photon energies near  $E_{\gamma} = 100$  GeV, corresponding to invariant energies of about  $\sqrt{s_{\gamma p}} \approx 14$  GeV. The GRV parametrizations of the parton densities [22] have been used. Since the average momentum fraction of the partons  $\langle \xi \rangle \sim 0.1$  is moderate, the curves are not sensitive to the parametrization in the small- $x$  region. The results are shown for two values

of  $\alpha_s^{(4)}(M_{J/\psi}^2) = 0.25$  and  $0.30$  which correspond to the average fit value in Ref.[23] and the  $1\sigma$  upper boundary of the error band, respectively. Since the cross section depends strongly on the QCD coupling, we adopt this measured value, thus allowing for a slight inconsistency to the extent that the GRV fits are based on a marginally lower value of  $\alpha_s$ . The  $K$ -factor  $K = \sigma_{\text{NLO}}/\sigma_{\text{LO}}$  turns out to be  $\sim 2.45$  with one part  $\sim 1.73$  due to the QCD radiative corrections of the leptonic  $J/\psi$  width and a second part  $\sim 1.44$  due to the dynamical QCD corrections *per se*. The  $K$ -factor is nearly independent of  $z$ . The dependence on the renormalization/factorization scale  $Q$  is reduced considerably in next-to-leading order [21]. While the ratio of the cross sections in leading order for  $Q = m_c : (\sqrt{2} m_c) : M_{J/\psi}$  is given by  $1.7 : 1.3 : 1$ , it is much closer to unity,  $0.9 : 1.1 : 1$ , in the next-to-leading order calculation, Fig.4. The overall behavior of the  $Q$  dependence is reminiscent of heavy quark production in hadron collisions [24]. The cross section runs through a maximum [25] near  $Q \approx 1.4 m_c$  with broad width, the origin of the stable behavior in  $Q$ . In the BLM scheme [26]  $Q$  moves from values below  $m_c$  at low energies up to  $\sim 1.5 m_c$  at the HERA energy of  $\sqrt{s_{\gamma p}} \approx 100$  GeV. In particular the value at high energies is significantly larger than the corresponding BLM value for  $J/\psi$  decays. The typical kinematical energy scale is not set any more by the small gluon energy in the  $J/\psi$  decay but rather by the typical initial-state parton energies.

In a systematic expansion we may finally add the relativistic corrections as estimated in Ref.[12]. Two conclusions can be drawn from the final results presented in Fig.3a. (i) The  $J/\psi$  energy dependence  $d\sigma/dz(\gamma + \mathcal{N} \rightarrow J/\psi + \mathcal{X})$  is adequately accounted for by the color-singlet model so that the shape of the gluon distribution in the nucleon can be extracted from  $J/\psi$  photoproduction data with confidence. (ii) The absolute normalization of the cross section is somewhat less certain; this is apparent from the comparison with the photoproduction data. [The situation is worse for electroproduction data [2]]. However, allowing for higher-twist uncertainties of order  $(\Lambda/m_c)^k \lesssim 20\%$  for  $k \geq 1$ , we conclude that the normalization too appears to be under semi-quantitative control – at the least.

In Fig.3b we present the prediction of the cross section for the HERA energy range. In this high energy range the  $K$ -factor is smaller than at low energies, a consequence of the negative dip in the  $c^{(1)}$  scaling function of Fig.2. For  $\alpha_s^{(4)}(M_{J/\psi}^2) = 0.25$  we find, for  $z < 0.9$ , a value of about  $\sigma(\gamma + p \rightarrow J/\psi + X) \approx 21$  nb at an invariant  $\gamma p$  energy of  $\sqrt{s_{\gamma p}} \approx 100$  GeV; this value rises to about 32 nb if we choose the larger value 0.30 for the QCD coupling. The production of  $\Upsilon$  bottomonium bound states is suppressed by a factor of about 300 at HERA, a consequence of the smaller bottom electric charge and the phase space reduction by the large  $b$  mass.

*In summa.* We have shown in this next-to-leading order perturbative QCD analysis that the energy shape of the cross section for  $J/\psi$  photoproduction is adequately described by the color-singlet model. A semi-quantitative understanding, at the least, has been achieved for the absolute normalization of the cross section. Higher-twist effects must be included to improve the quality of the theoretical analysis further. The predictions for the HERA energy range provide a crucial test for the underlying picture as developed so far in the perturbative QCD sector.

## Acknowledgements

We have benefitted from discussions with S.J. Brodsky, J.H. Kühn, G. Schuler and W. van Neerven. Special thanks go to W. Beenakker, V. Del Duca and M. Spira for their continuous advice in solving  $\epsilon$  problems. Last but not least, discussions on photo- and electroproduction data with H. Jung and J.N. Lim are gratefully acknowledged. MK would like to thank J.G. Körner for discussions and support.

## References

- [1] E.L. Berger and D. Jones, Phys. Rev. D23 (1981) 1521; R. Baier and R. Rückl, Phys. Lett. 102B (1981) 364.
- [2] H. Jung, G.A. Schuler and J. Terrón, Int. J. Mod. Phys. A7 (1992) 7955; A. Ali, Report DESY 93-105.
- [3] M.G. Ryskin, Z. Phys. C57 (1993) 89; J.R. Forshaw and M.G. Ryskin, Report DESY 94-162; J.R. Cudell, Nucl. Phys. B336 (1990) 1.
- [4] T. Ahmed et al. [H1 Collaboration], Phys. Lett. 338B (1994) 507.
- [5] A.D. Martin, C.-K. Ng and W.J. Stirling, Phys. Lett. 191B (1987) 200.
- [6] H. Jung, J.N. Lim, private communication.
- [7] E. Braaten, M.A. Doncheski, S. Fleming and M.L. Mangano, Phys. Lett. 333B (1994) 548; M. Cacciari and M. Greco, Phys. Rev. Lett. 73 (1994) 1586.
- [8] R. Barate et al. [NA-14 Collaboration], Z. Phys. C33 (1987) 505.
- [9] B.H. Denby et al. [FTPS Collaboration], Phys. Rev. Lett. 52 (1984) 795.
- [10] J.J. Aubert et al. [EMC Collaboration], Nucl. Phys. B213 (1983) 1.
- [11] D. Allasia et al. [NMC Collaboration], Phys. Lett. 258B (1991) 493.
- [12] H. Jung, D. Krücker, C. Greub and D. Wyler, Z. Phys. C60 (1993) 721.
- [13] G.T. Bodwin, E. Braaten and G.P. Lepage, Preprint ANL-HEP-PR 94-24 (1994).
- [14] W. Beenakker, H. Kuijf, W. van Neerven and J. Smith, Phys. Rev. D40 (1989) 54.
- [15] W.A. Bardeen, A.J. Buras, D.W. Duke and T. Muta, Phys. Rev. D18 (1978) 3998.
- [16] J. Collins, F. Wilczek and A. Zee, Phys. Rev. D18 (1978) 242; W.J. Marciano, Phys. Rev. D29 (1984) 580; P. Nason, S. Dawson and R.K. Ellis, Nucl. Phys. B303 (1988) 607.
- [17] A. Sommerfeld, *Atombau und Spektrallinien*, Vieweg 1939; I. Harris and L.M. Brown, Phys. Rev. 105 (1957) 1656.

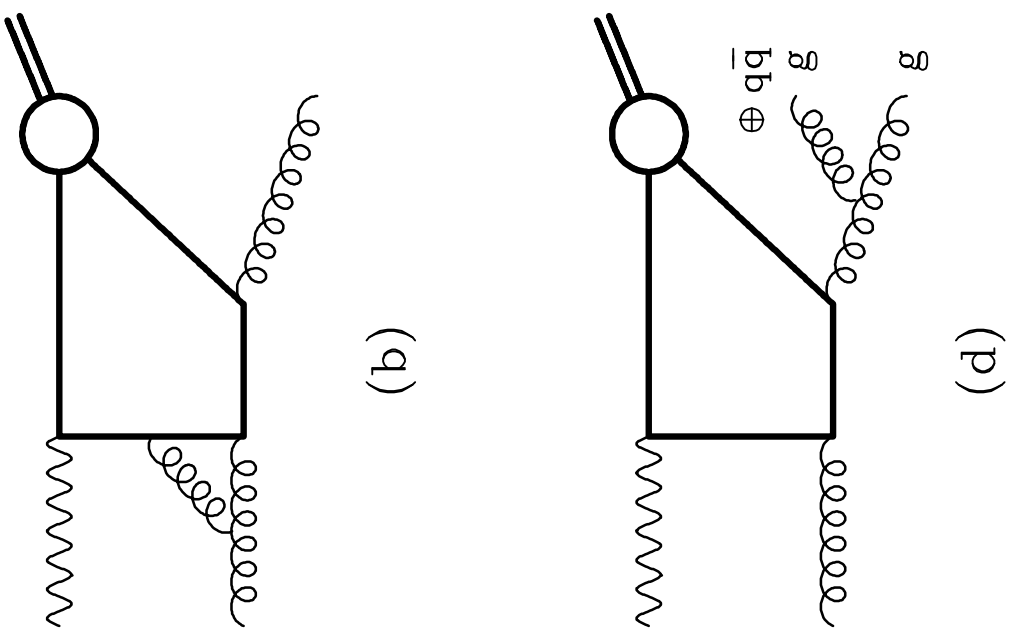
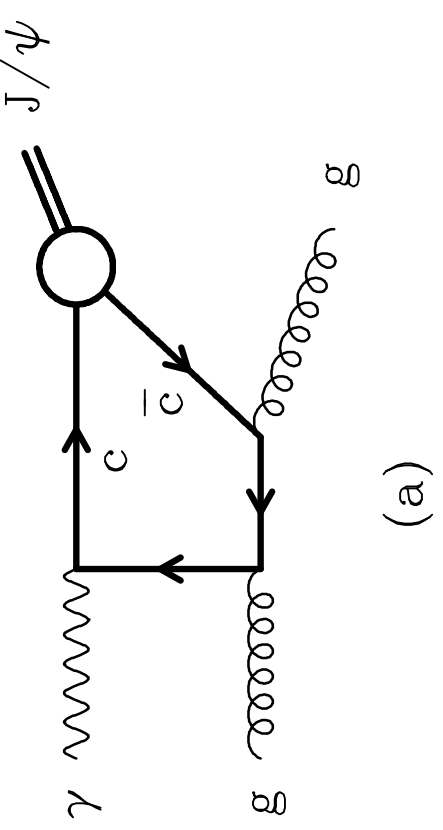
- [18] J. Smith and W. van Neerven, Nucl. Phys. B374 (1992) 36.
- [19] G. Altarelli, R.K. Ellis and G. Martinelli, Nucl. Phys. B157 (1979) 461.
- [20] R. Barbieri, R. Gatto and E. Remiddi, Phys. Lett. 106B (1981) 497.
- [21] M. Krämer, PhD. Thesis, Univ. of Mainz, 1994; J. Zunft, PhD. Thesis, Univ. of Hamburg, 1994.
- [22] M. Glück, E. Reya and A. Vogt [GRV], Z. Phys. C53 (1992) 127.
- [23] S. Bethke, Proceedings Tennessee Int. Symposium on Radiative Corrections, Gatlinburg; Aachen Report PITHA 94-24.
- [24] G. Altarelli, M. Diemoz, G. Martinelli and P. Nason, Nucl. Phys. B308 (1988) 724.
- [25] P.M. Stevenson, Phys. Rev. D23 (1981) 2916.
- [26] S.J. Brodsky, G.P. Lepage and P.B. Mackenzie, Phys. Rev. D28 (1983) 228.

## Figures

- Fig. 1. Generic diagrams for inelastic  $J/\psi$  photoproduction: (a) leading order contribution; (b) vertex corrections; (c) box diagrams; (d) splitting of the final state gluon into gluon or light quark-antiquark pairs; (e) diagrams renormalizing the initial-state parton densities.
- Fig. 2. (a) Coefficients of the QCD corrected total inelastic [ $z < 0.9$ ] cross section  $\gamma + g \rightarrow J/\psi + X$  in the physically relevant range of the scaling variable  $\eta = s_{\gamma p}/4m^2 - 1$ ; and (b) for  $\gamma + q/\bar{q} \rightarrow J/\psi + X$ .
- Fig. 3. (a) Energy spectrum  $d\sigma/dz$ , at the initial photon energy  $E_\gamma = 100$  GeV, for two different values of  $\alpha_s(M_{J/\psi}^2)$  compared with the photoproduction data [8,9]. (b) Total cross section for inelastic  $J/\psi$  photoproduction  $\gamma + P \rightarrow J/\psi + X$  as a function of the photon-proton center of mass energy in the HERA energy range. [The dashed line presents the  $\Upsilon$  photoproduction cross section, amplified by a factor 100.]
- Fig. 4. Dependence of the total cross section  $\gamma + g \rightarrow J/\psi + X$  on the renormalization/factorization scale  $Q$  at a photon energy of  $E_\gamma = 100$  GeV.

This figure "fig1-1.png" is available in "png" format from:

<http://arxiv.org/ps/hep-ph/9411372v1>



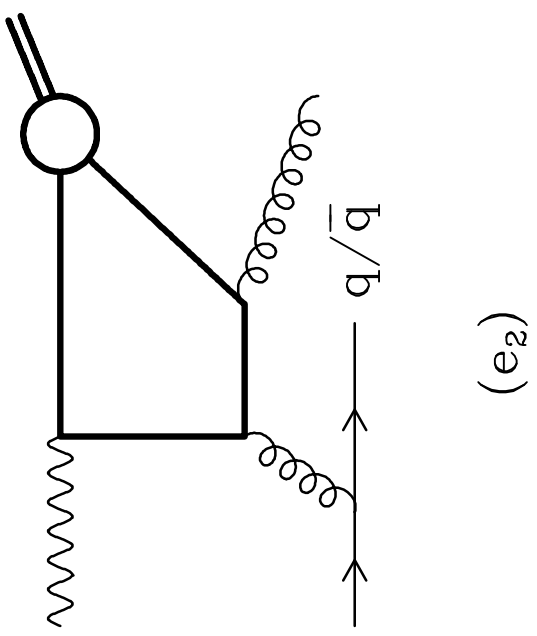
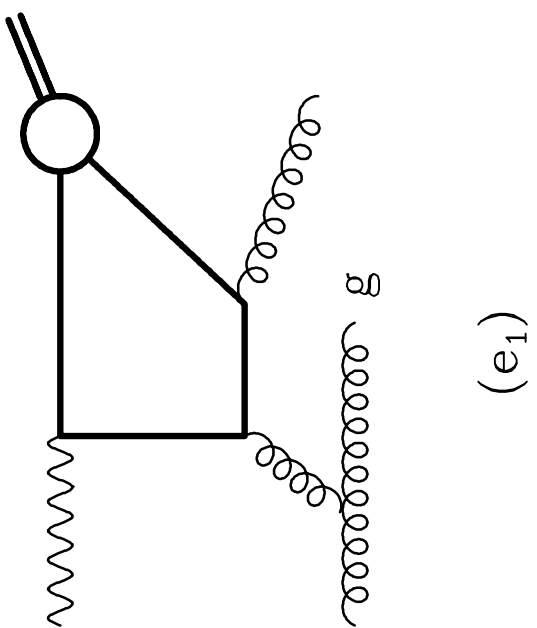
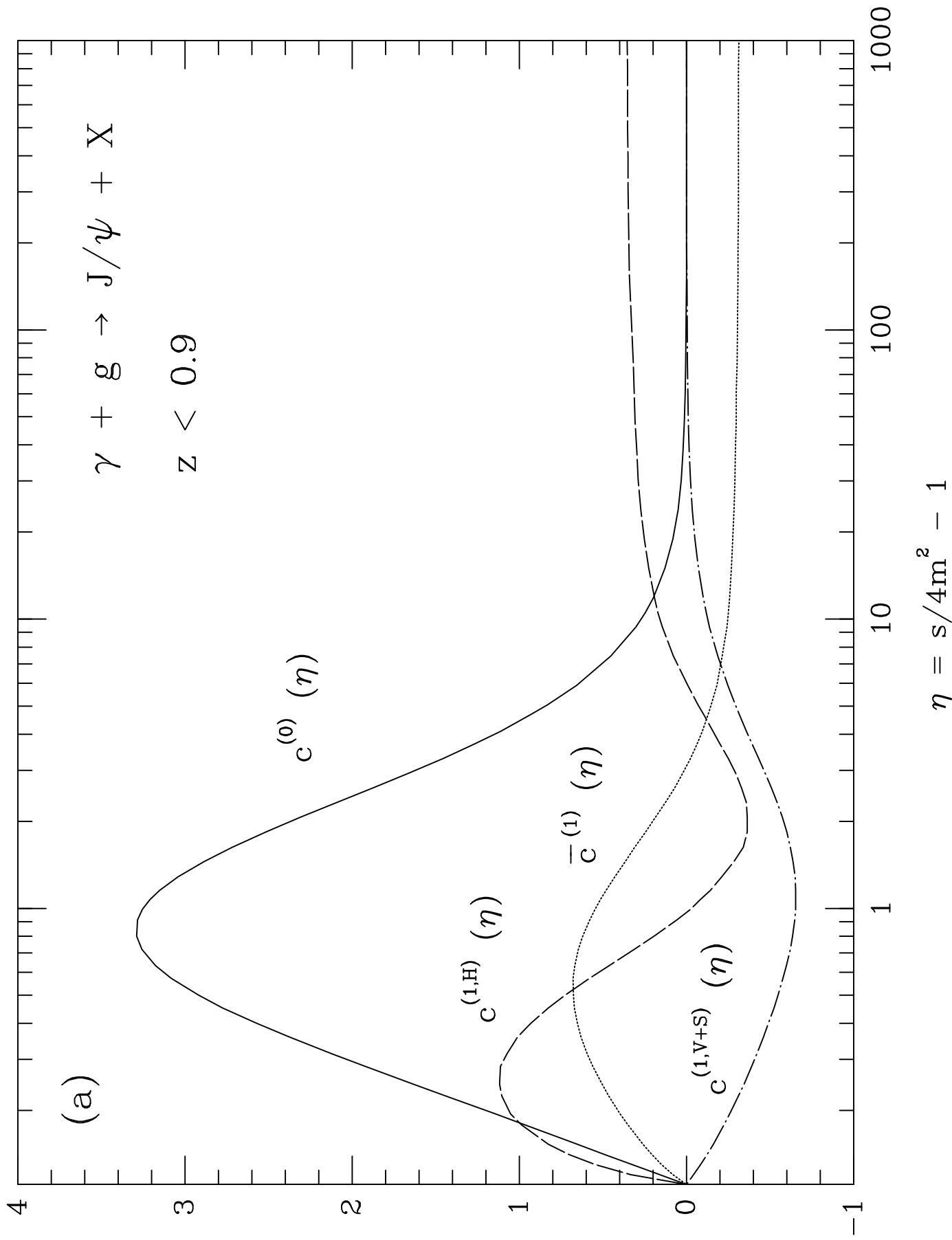


Fig. 1



This figure "fig1-2.png" is available in "png" format from:

<http://arxiv.org/ps/hep-ph/9411372v1>



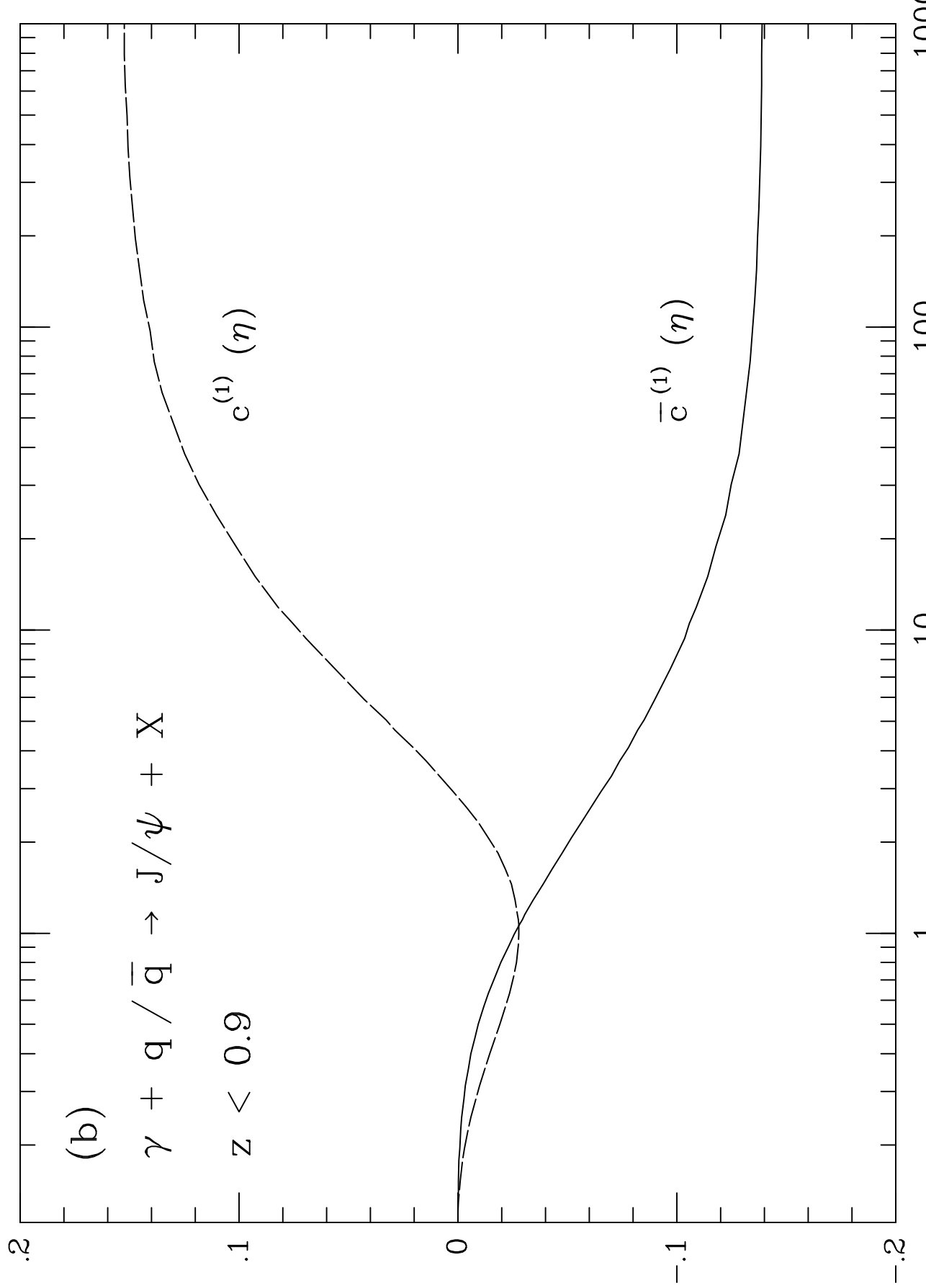
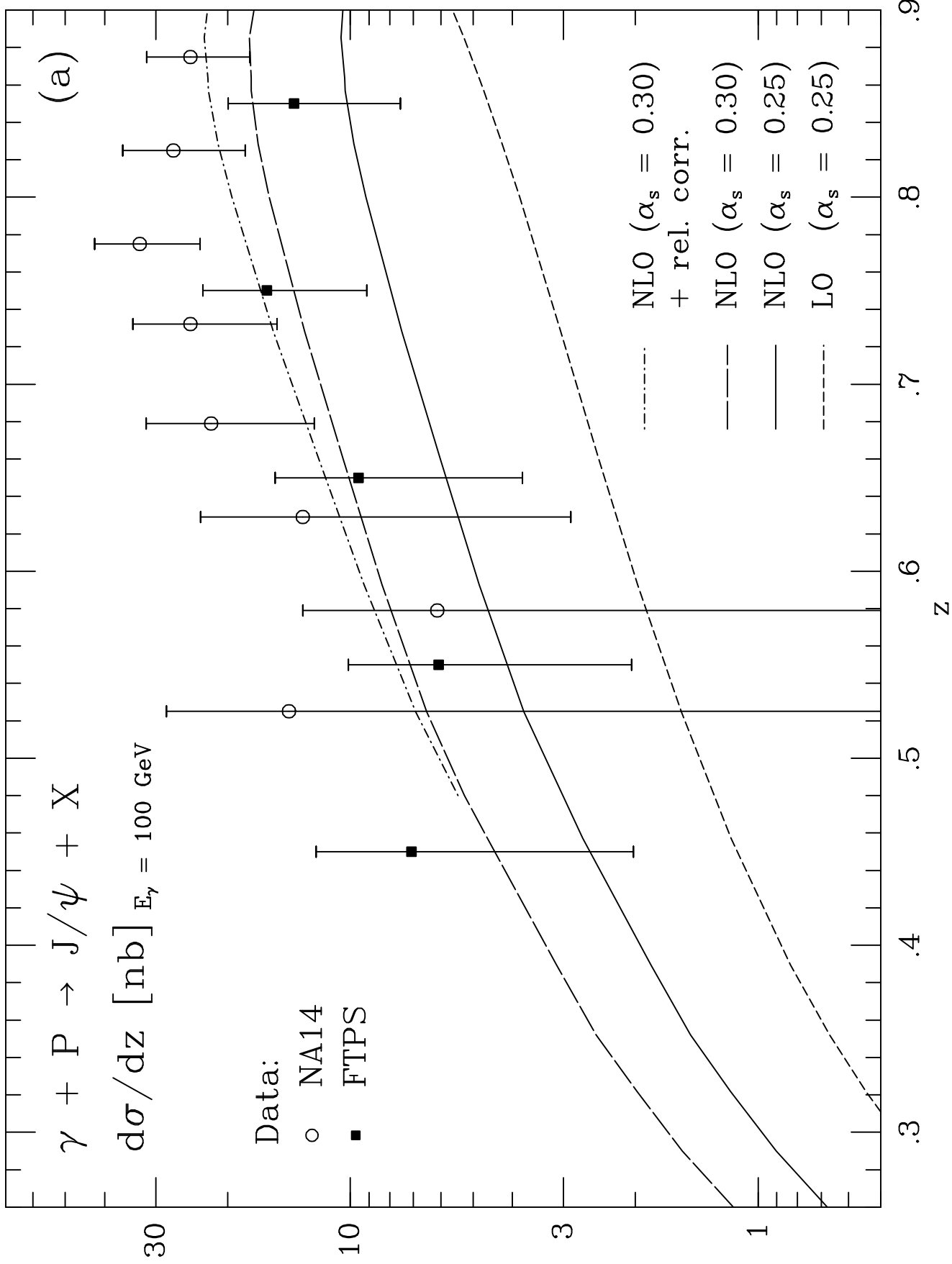


Fig. 2  
 $\eta = s/4m^2 - 1$

This figure "fig1-3.png" is available in "png" format from:

<http://arxiv.org/ps/hep-ph/9411372v1>



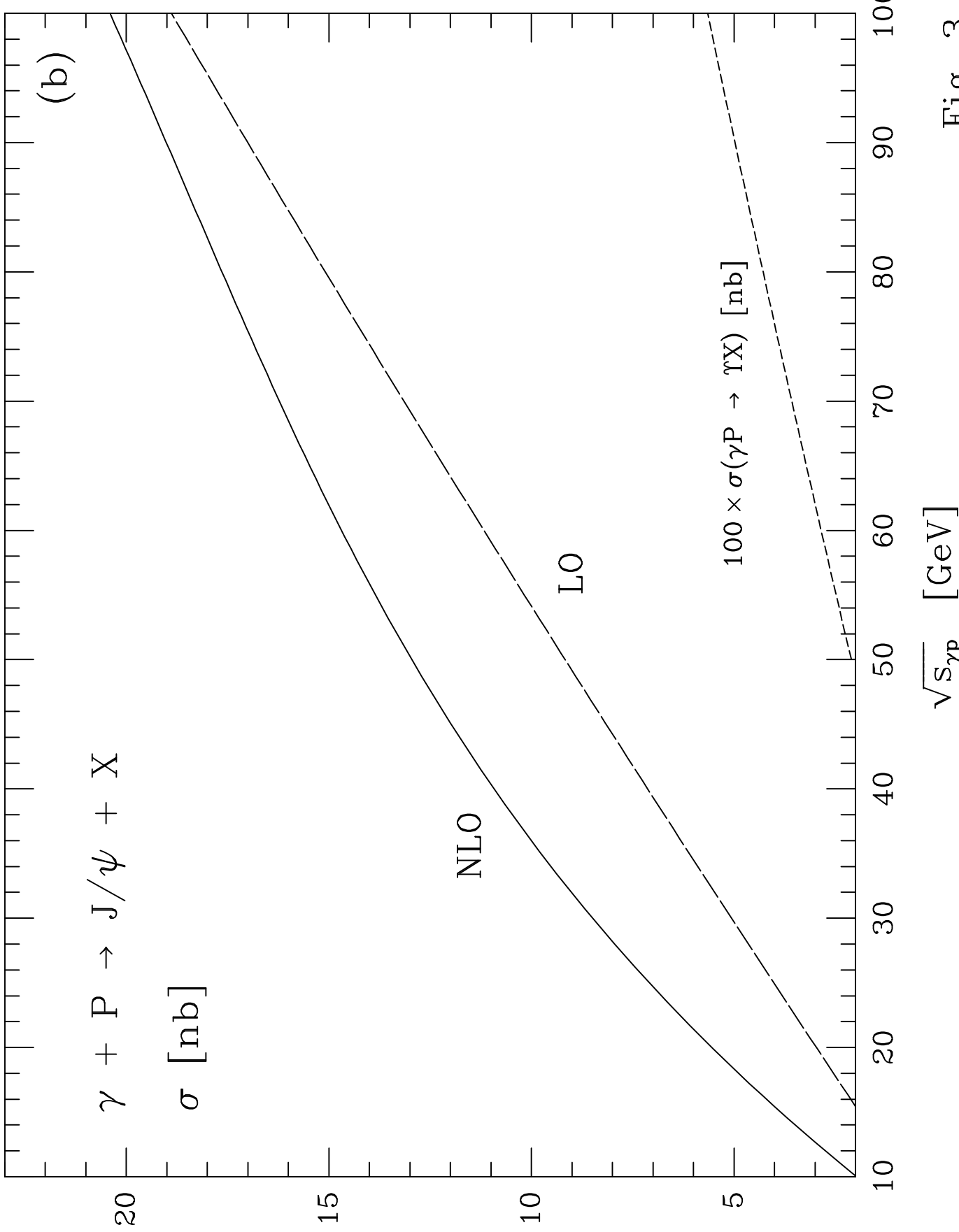


Fig. 3

This figure "fig1-4.png" is available in "png" format from:

<http://arxiv.org/ps/hep-ph/9411372v1>

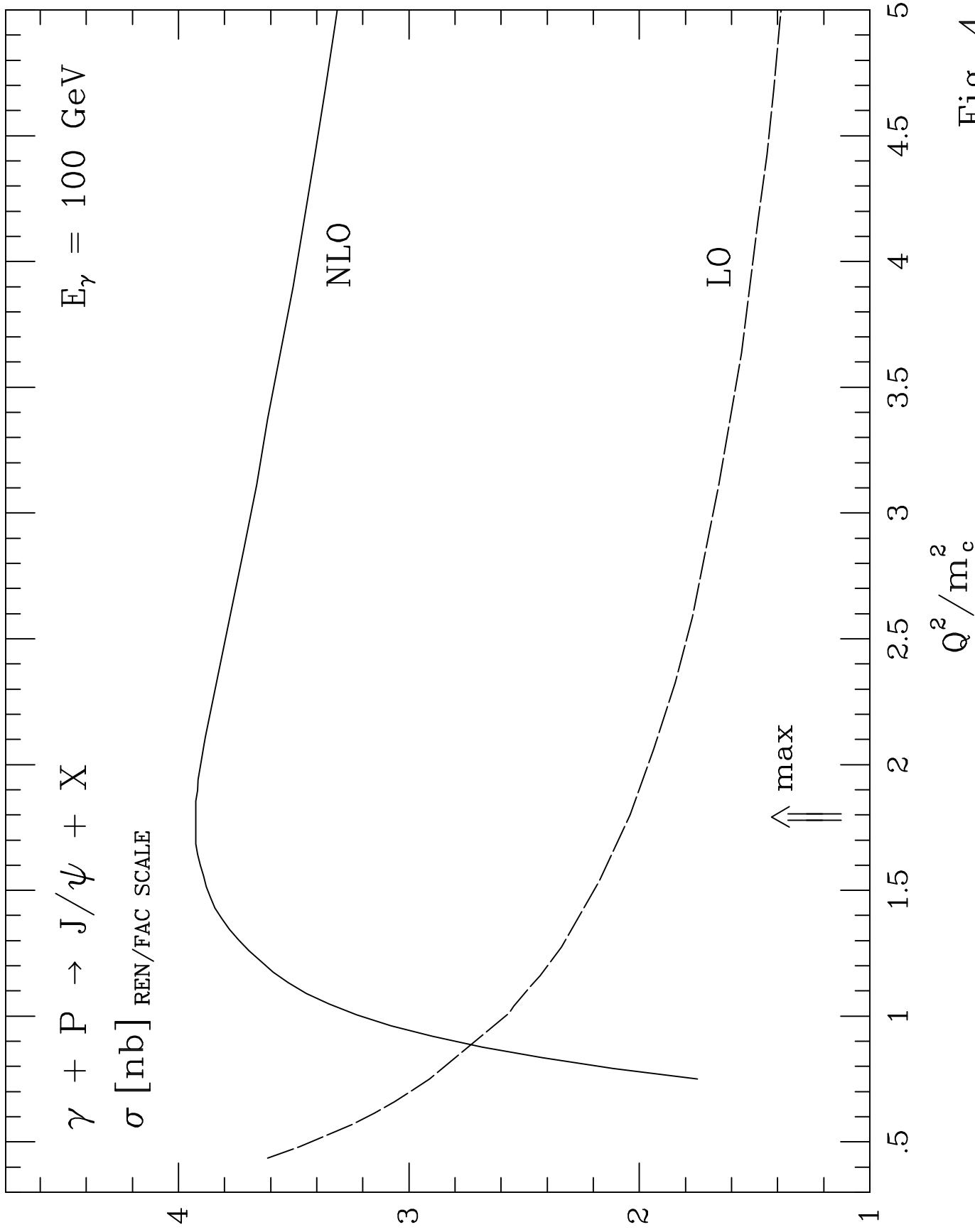


Fig. 4

This figure "fig1-5.png" is available in "png" format from:

<http://arxiv.org/ps/hep-ph/9411372v1>

This figure "fig1-6.png" is available in "png" format from:

<http://arxiv.org/ps/hep-ph/9411372v1>

This figure "fig1-7.png" is available in "png" format from:

<http://arxiv.org/ps/hep-ph/9411372v1>